Microchimica Acta (2019) 186:518
https://doi.org/10.1007/s00604-019-3599-y

ORIGINAL PAPER

Copper(II)-coated Fe_3O_4 nanoparticles as an efficient enzyme mimic for colorimetric detection of hydrogen peroxide

Hongying Liu[1] · Langlang Zhu[1] · Huan Ma[1] · Jiajun Wen[1] · Hanxiao Xu[1] · Yubing Qiu[1] · Linan Zhang[1] · Lihua Li[1] · Chunchuan Gu[2]

Received: 29 December 2018 / Accepted: 10 June 2019
© Springer-Verlag GmbH Austria, part of Springer Nature 2019

Abstract

The authors describe the preparation of Cu(II)-coated Fe_3O_4) nanoparticles (NPs) that possess excellent peroxidase-like activity. The NPs were formed by chelation between Cu(II) ions and the oxygen functional groups of sodium ligninsulfonate. The morphology and structure of the NPs were characterized by scanning electron microscopy, transmission electron microscopy, X-ray powder diffraction, X-ray photoelectron spectroscopy, and Fourier transform infrared spectroscopy. The NPs have an average diameter of 220 nm. They are shown to be viable peroxidase mimics that can catalyze the oxidation of 3,3′,5,5′-tetramethylbenzidine by hydrogen peroxide to produce a blue coloration. The findings were used to design a colorimetric assay that has a linear response in the 2.5 to 100 μM H_2O_2 concentration range and a 0.2 μM detection limit. The assay excels by its selectivity, high sensitivity, good selectivity, portability and cost efficiency.

Keywords Fe_3O_4-Cu^{2+} nanoparticles · Nanozyme · Biosensor · Hydrogen peroxide · Colorimetric method

Introduction

Hydrogen peroxide (H_2O_2) is a reactive molecule that plays a major role in many fields such as the biological, chemical, pharmaceutical, food and environmental sciences [1, 2]. Thus, it is particularly important to establish sensitive and selective methods for the determination of H_2O_2. For this aim, colorimetric means have been used because of their unique advantages, such as fast response, simple operation, low cost and high sensitivity [3]. Thereinto, nanoparticle-based enzyme mimics, named nanozymes, have attracted great attention as an ideal transducer of colorimetry for sensing of H_2O_2 with their advantages of cheap cost and good stability [4]. It not only has unique physical and chemical properties of nanomaterials, but also has the catalytic activity of natural enzymes. In recent years, with the rapid development of nanomaterials, nanozymes researches have been growing at an exponential rate.

Yang et al. have found that magnetic iron oxide nanoparticles (MNPs) exhibited an intrinsic enzyme mimetic property [5]. It was recognized as one of the earliest to be discovered. Compared to traditional natural enzymes, the MNPs nanozymes have several excellent advantages. First, MNPs has powerful magnetic properties that can satisfy magnetic separation and enrichment. Secondly, compared to HRP, the catalytic activity of MNPs is more stable therefore the reactionary conditions can be controlled. Thirdly, the preparation and purification of MNPs are affordable [6]. Over the past decade, MNPs have been applied in several fields, such as biological catalysis and separation, magnetic resonance imaging, drug delivery, and so on [7–9] due to advantages that include large surface area, a great amount of active sites, and strong magnetic activity [10]. The enzymes or mental catalysts were coated on the surface of magnetic nanoparticles to form functional nanomaterials for improving their catalytic characteristics [11–14]. However, due to the complicated preparation

Electronic supplementary material The online version of this article (https://doi.org/10.1007/s00604-019-3599-y) contains supplementary material, which is available to authorized users.

✉ Linan Zhang
zln@hdu.edu.cn

✉ Lihua Li
lilh@hdu.edu.cn

✉ Chunchuan Gu
gcc5413@163.com

[1] Hangzhou Dianzi University, Hangzhou 310018, China

[2] Deparment of Clinical Laboratory, Hangzhou Cancer Hospital, Hangzhou 310002, China

Published online: 09 July 2019

process and high cost, they have not been widely used. Thus, it is crucial to develop a facile and cheap method for the preparation of nanozymes with high catalytic activity and strong magnetic properties.

Notably, copper ions are one of the earliest metals used by mankind. They are commonly existing active sites in natural enzymes. Despite this, few studies based on copper ion's nanozyme such as Cu^{2+}-modified carbon nitride, Cu^{2+}-modified carbon dots, Cu^{2+}-modified graphene oxide, and Cu^{2+}-modified metal-organic framework nanoparticles, copper(II)-poly-L-histidine functionalized multi-walled carbon nanotubes have been reported [15–22]. In this regard, the combination of magnetic nanoparticles with Cu(II) has considerable application prospects for the study of nanozymes.

Inspired by the above requirements, we employed an adsorption method for the synthesis of copper(II) coated Fe_3O_4 nanocomposite (Fe_3O_4-Cu^{2+}), as shown in Scheme 1. We also demonstrated that Fe_3O_4-Cu^{2+} NPs possess excellent peroxidase-like catalytic properties and strong magnetism. The catalytic mechanism was also within the scope of our research. Finally, as a proof-of-concept, Fe_3O_4-Cu^{2+} NPs were used to design a sensitive colorimetric method for detecting H_2O_2.

Experimental

Reagents

Iron(III) chloride hexahydrate and TMB were acquired from Sangon Biotech Co., Ltd. (China, www.sangon.com). H_2O_2 (30%), hydrochloric acid and copper nitrate was produced by Sinopharm Chemical Reagent Co., Ltd. (China, en.reagent.com.cn). Furthermore, it was from Aladdin Industrial Co., Ltd. (China, www.aladdin-e.com) that we purchased sodium hydroxide, sodium acetate trihydrate and ethylene glycol. Sodium ligninsulfonate (SL) was provided by the Tianjin Guangfu Fine Chemical Research Institute (tjguangfu.bioon.com.cn, CAS: 8061-51-6). In addition, a Millipore Milli-Q system (18.2 MΩ cm) supplied the experimental water. The HAc-NaAc buffer (0.1 M) with pH value range between 2 and 12 was obtained using variant proportions of 0.1 M HAc as well as 0.1 M NaAc solution.

Instruments

Under conditions of an acceleration voltage of 200 kV, the images of transmission electron microscopy (TEM) were generated by a Tecnai G2 F20 S-TWIN (FEI, America, www.fei.com) electron microscope. It was a JSM-7500 field emission scanning electron microscope with an EDX spectrometer that we used to take images of field emission scanning electron microscopy (FESEM). We use the method of dropping a dispersed solution onto an ITO slide and placing the ITO slides on a copper disc and a copper film, respectively, and then drying in air to prepare the SEM and TEM analysis samples. The spectra of Fourier transform infrared (FTIR) was measured on the Nicolet Nexus FTIR model 670 Spectrometer (Thermo, America, www.americanthermoform.com) in the range of 400 to 4000 cm^{-1}. We use X-ray diffraction (XRD) on a MinFlex600 X-ray diffractometer to test the nanomaterial crystalline phase (www.rigaku.com). The measurement of X-ray photoelectron spectroscopy (XPS) was on ESCALab250 (Thermo, America, www.americanthermoform.com). It was a UV-3600 spectrophotometer (Shimadzu, Kyoto, Japan, www.shimadzu.com) or a Varioskan Flash spectrometer (Thermo Fisher Scientific, America, www.thermofisher.com) that used to conduct the spectra of UV-visible absorption.

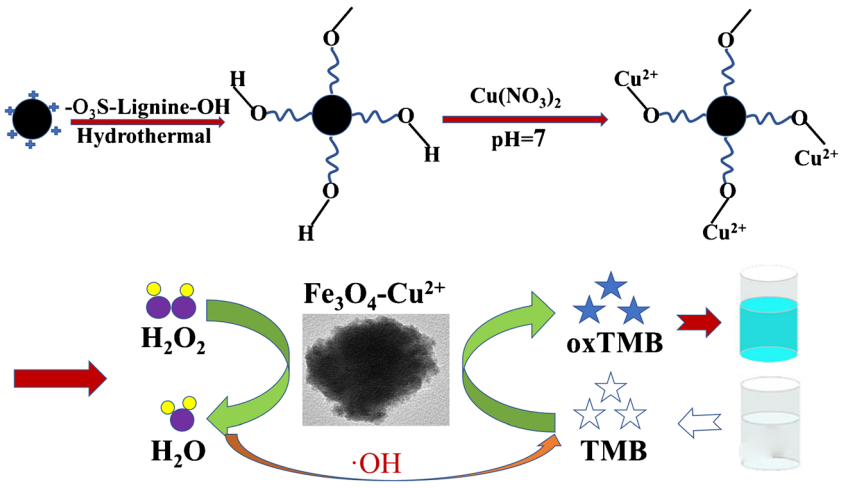

Scheme 1 Schematic diagram of the preparation technology for Fe_3O_4-Cu^{2+} NPs and colorimetric nanoprobe for H_2O_2

Synthesis of Fe_3O_4-Cu^{2+} nanoparticles

Fe_3O_4-Cu^{2+} nanoparticles were prepared via a two-step method. Firstly, Fe_3O_4-SL was synthesized via a simple alcohol-thermal process which was described previously [23, 24]. Detailed procedures are included in the Supporting Information.

Hereafter, 0.02 g Fe_3O_4-SL was added into 50 mL 0.5 g·L^{-1} Cu^{2+} solution under neutral conditions (pH = 7) and mixed thoroughly. Then, the solution was taken into a three-necked flask at the mechanical stirring rate of 400 r/min at 25 °C for 3 h. The product needs to be processed in three steps: the first step was centrifuged, the second part was washed three times with ultrapure water, and the third step is dried at 50 °C for 8 h, which can achieve the final product.

General procedure for assessing peroxidase-like activity

Since the peroxidase mimetic activity of Fe_3O_4-Cu^{2+} NPs was researched, the catalytic oxidation of the peroxidase substrate TMB that had H_2O_2 was measured. The catalytic experiment was conducted as follows: a mixture consists of 50 μL Fe_3O_4-Cu^{2+} NPs (25 μg mL^{-1}), 50 μL H_2O_2 (25 mM), 1850 μL HAc-NaAc (pH = 3, 0.1 M) and 50 μL TMB (0.8 mM) was incubated 30 min at 25 °C. Then, we recorded spectrum of UV-Vis absorption at 652 nm. In addition, the effect of the reaction temperature (15~75 °C), the pH of the buffer (2~12) and concentration of Fe_3O_4-Cu^{2+} NPs (2–18 μg mL^{-1}) on the peroxidase mimetic activity of Fe_3O_4-Cu^{2+} NPs were researched to achieve the optimal condition for a Fe_3O_4-Cu^{2+} NPs detection system.

Steady-state kinetics analysis

To further find out the steady-state kinetics of Fe_3O_4-Cu^{2+} NPs, the two most important kinetic parameters were calculated through many experiments: K_m and V_m. First of all, keeping the concentration of TMB (0.4 and 0.8 mM) constant and varying the H_2O_2 concentration (0.6–10 mM), the mixture solution consisted of a HAc-NaAc buffer (1850 μL, 0.1 M, pH = 3) and Fe_3O_4-Cu^{2+} NPs (50 μL, 25 μg mL^{-1}). TMB and H_2O_2 were prepared and reacted 35 min at 45 °C. At last, we detailed the absorbance of the mixture of 652 nm. Similarly, solutions used for kinetic analysis with H_2O_2 as the substrate was studied by maintaining the H_2O_2 concentration and changing the TMB concentration under the same conditions.

The Lineweaver-Burk plot derived from the Michaelis-Menten equation was carried out to calculate the enzyme kinetic parameters: $\frac{1}{V} = K_m/V_{max}(1/[s] + 1/K_m)$. In this formula, v represents the reaction rate; V_{max} represents the maximum reaction rate; [s] represents the substrate concentration, and K_m represents the Michaelis constant [25]. Herein, the Ox-TMB concentration is quantitatively counted according to Lambert-Beer Law (A = kbc), where, A is absorbance, b represents the solution's thickness, c is the Ox-TMB concentration, and k stands for the molar absorption coefficient which was usually considered to be 39,000 cm^{-1} [26].

Colorimetric determination of H_2O_2

The process of H_2O_2 detection was performed as follows: At first, TMB (50 μL, 0.8 mM) and Fe_3O_4-Cu^{2+} nanoparticles (25 μg mL^{-1}, 50 μL) were placed successively into a mixed buffer for sodium acetate (1900 μL, pH = 3) containing different H_2O_2 concentrations. Then, incubate the above solution 35 min at 45 °C, the adsorption spectroscopy was scanned from 400 to 800 nm. Finally, we recorded the integrated absorbance at 652 nm and thus a linear equation of H_2O_2 concentration was established.

Results and discussion

Choice of materials

It is well known that a lot of nanomaterials such as MNPs, noble NPs, and carbon NPs have been reported to have intrinsic enzyme mimetic property [27–29]. Among them, MNPs are the most widely used materials which combine magnetic separation with enzymatic properties. However, they have poor water solubility, easy agglomeration, and large particle size, resulting in a great limitation on their catalytic activity. Ionic liquid dopamine were used to modify MNPs to improve solve this problem. SL is a natural high molecular polymer with non-toxic, biodegradable properties and is rich in functional groups, including methoxy, hydroxyl, sulfonic acid groups and etc. Furthermore, copper ion is proved to be a good mimetic property. And copper ions could modify on the surface by SL. Therefore, Fe_3O_4-Cu^{2+} NPs were synthesized and employed to fabricate colorimetric method for the determination of H_2O_2.

Characterization of Fe_3O_4-SL and Fe_3O_4-Cu^{2+} NPs

As mentioned before, Fe_3O_4-Cu^{2+} NPs were synthesized through two steps. First, Fe_3O_4-SL NPs were synthesized by the alcohol-thermal method using SL as surfactant. Then, Fe_3O_4-Cu^{2+} NPs are formed by reacting the Fe_3O_4-SL particles with Cu^{2+} ions. The SL containing various oxygen functional groups are responsible for the formation of

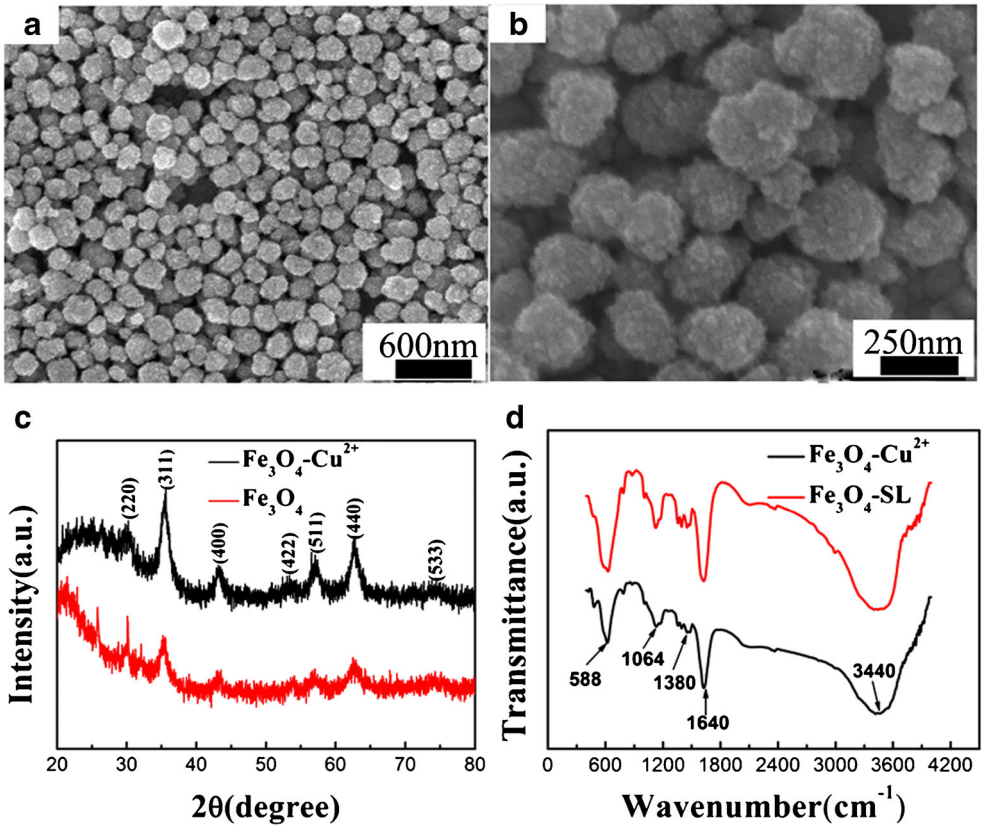

Fig. 1 SEM images of Fe_3O_4-SL NP (**a**), Fe_3O_4-Cu^{2+} NPs (**b**), and XRD spectrum (**c**) of Fe_3O_4-Cu^{2+} NPs, FTIR pattern of Fe_3O_4-SL NPs and Fe_3O_4-Cu^{2+} NPs (**d**)

nanoparticles with Cu^{2+}. To verify the successful preparation of Fe_3O_4-Cu^{2+} NPs, a series of measurements including SEM, TEM, XRD, FTIR, EDS and XPS were carried out.

SEM and TEM were first used to characterize the morphology of Fe_3O_4-Cu^{2+} NPs. Figure 1a shows that the monodisperse Fe_3O_4-SL NPs consist of spherical structures with average sizes of 125 nm in diameter. SL absorbed on the surface of Fe_3O_4 is rich in $RCOO^-$ groups. This makes Fe_3O_4 nanoparticles surrounded by negative charges. The particles have good dispersibility due to electrostatic and steric effects. After Cu^{2+} was modified on the surface of Fe_3O_4-SLNPs, Fe_3O_4-Cu^{2+} NPs generally maintain the spherical structure and good dispersion of Fe_3O_4-SL nanoparticles with the average size of 220 nm (Fig. 1b and S1a). Then, the crystal structures of Fe_3O_4-SL and Fe_3O_4-Cu^{2+} NPs were investigated by XRD as shown in Fig. 1c. All observed diffraction peaks correspond to the reported Fe_3O_4 phase (JCPDS 75–1609). The peaks of 2θ at 30.07°,35.41°, 37.01°, 43.01°, 53.29°, 62.49°, 73.90° corresponding to Fe_3O_4 crystal planes (220), (311), (222), (400), (422), (511), (440), (533), respectively. This result illustrates that synthesized materials possess a cubic spinel structure.

Subsequently, FTIR spectra were executed for the investigation of the structure and components of Fe_3O_4-Cu^{2+} NPs. Figure 1d clearly shows the results. Before Cu^{2+} doping, the Fe_3O_4-SL NPs show a broad and strong peak at 3440 cm^{-1} and five strong peaks at 2960, 1640, 1380, 588, and 580, which belongs to a benzene ring C-H stretching vibrations, O-H stretching vibrations, telescopic vibration of a benzene ring, S=O vibration, and Fe-O. This indicates that SL has successfully modified on the surface of Fe_3O_4 nanoparticles. As for curve Fe_3O_4-Cu^{2+} NPs the absorption band of O-H and Fe-O becomes narrower and weaker due to the chelation reaction between Cu^{2+} and -O-H, indicating successful preparation of Fe_3O_4-Cu^{2+} nanoparticles.

Moreover, the chemical component and state were studied by EDS and XPS. As demonstrated in Fig. S1b, the elements of Cu, Fe, O and S coexisted in the nanoparticles, verifying the existence of Cu. The S peak comes from the modification of SL, while Cu and Fe belong to the chelation of Cu^{2+} and Fe_3O_4. The O peak is attributed to Fe_3O_4 and SL. The measurements of XPS provided further proof of the Fe_3O_4-Cu^{2+} nanoparticles. The XPS result support the direct evidence of Cu^{2+} in the Fe_3O_4-SL and the state of oxidation, degree of adaptability and chemical constitution. As shown in Fig. S2a, the peaks of C1s, O1s, S2p, Fe2p, Cu2p are clearly observed in the full scan spectrum, further indicating C, O, S, Fe, Cu atoms formed the Fe_3O_4-Cu^{2+} NPs. To investigate the

oxidation state of copper in our prepared Fe_3O_4-Cu^{2+} nanoparticles, the spectra of Cu2p and CuLMM were analyzed. In Fig. S2b, Cu2p3/2 and Cu2p1/2 electrons of Cu^{2+} corresponded two highest points at 933.5 and 953.4 eV, respectively [21]. Moreover, another two peaks located at 941.95 and 962.05 eV belonging to the d9 configuration in the ground state of Cu^{2+} are observed, indicating the paramagnetic chemical state of Cu^{2+} [22]. The peak of Cu^{+} located at 572.9 eV can be observed in Fig. S2c. It proves the presence of Cu^{+} [20]. Therefore, part of Cu^{2+} is changed to the original Cu^{+} during the formation of Fe_3O_4-Cu^{2+} NPs, and thus leads to higher activity. All of these indicate that Cu^{2+} was successfully doped in Fe_3O_4 nanoparticles.

Peroxidase-like activity of the Fe_3O_4-Cu^{2+} NPs

It is known that, Fe_3O_4 and Cu^{2+} exhibit excellent peroxidase-like activity. Thus, we predict that our designed NPs also have good catalytic properties. Since the Fe_3O_4-Cu^{2+} NPs peroxidase-like activity investigated, under the circumstance of presence of H_2O_2, we formed a critical opinion of the catalytic oxidized chromogenic peroxidase substrate TMB. Figure 2A shows that the NPs can catalytically oxidize colorless TMB to blue colored oxidized TMBox which has an absorption maximum at 652 nm. However, the absence of H_2O_2 or TMB generated ignorable color changes. Moreover, a time curve of different reaction systems within 50 min was carried out by determining the absorbance changes in the conditions of 652 nm. In Fig. 2B, the relative activity of the Fe_3O_4-Cu^{2+}-TMB and Fe_3O_4-Cu^{2+}-H_2O_2 systems are significantly lower than that of the Fe_3O_4-Cu^{2+}-TMB-H_2O_2 system. This shows that Fe_3O_4-Cu^{2+} can catalyze the oxidation of H_2O_2 to generate ·OH radicals, allowing·OH species to catalyze TMB oxidizing to generate a distinct color change [30]. There is excellent peroxidase-like catalytic activity in the NPs. There are enough active sites which are provided by the spherical structure for the catalytic oxidation TMB. Furthermore, the catalytic activity of Fe_3O_4, Cu^{2+} and Fe_3O_4-Cu^{2+} NPs was compared. From Fig. 2C, we can find that under the same conditions, the color change of Fe_3O_4 or Cu^{2+} reaction system is weaker than that of Fe_3O_4-Cu^{2+} NPs reaction system with obvious color change. The maximum reaction relative activity shown in Fig. 2D is approximately three times and two times larger than Fe_3O_4 and Cu^{2+} respectively, demonstrating a higher peroxidase-like activity of the Fe_3O_4-Cu^{2+} nanomaterial derived from the synergetic coupling effect between Fe_3O_4 and Cu^{2+}.

Optimization of method

The following parameters were optimized: (a) sample pH value; (b) reaction temperature; (c) Fe_3O_4-Cu^{2+} NP concentration; (d) reaction time. Respective data and Figures are given in the Electronic Supporting Materials. The following

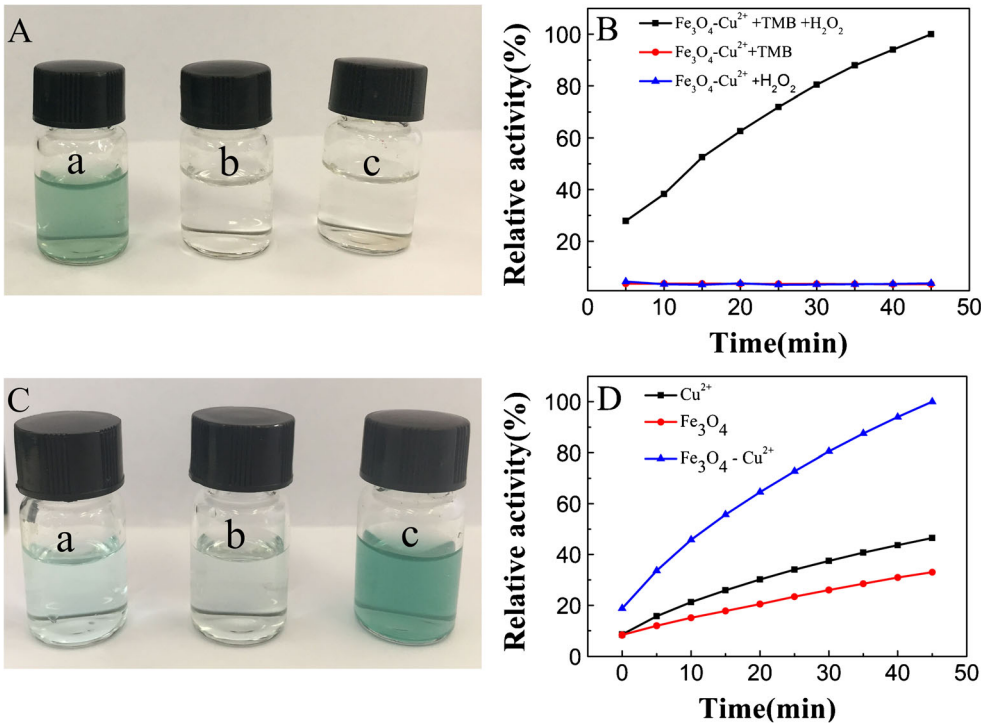

Fig. 2 (**A**) Photographs and (**B**) the absorbance changes within 0–45 min at 652 nm of different reaction systems: Fe_3O_4-Cu^{2+} + TMB + H_2O_2 (a), Fe_3O_4-Cu^{2+} + TMB (b) and Fe_3O_4-Cu^{2+}+H_2O_2 (c). (**C**) Photographs and (**D**) the absorbance changes within 0–45 min in the conditions of 652 nm of variant reaction hierarchy: Cu^{2+}+TMB + H_2O_2 (a), Fe_3O_4 + TMB + H_2O_2 (b) and Fe_3O_4-Cu^{2+}+TMB + H_2O_2 (c). Conditions for completion of the experiment: operation was carried out in acetate buffer of (pH = 3) at 25 °C

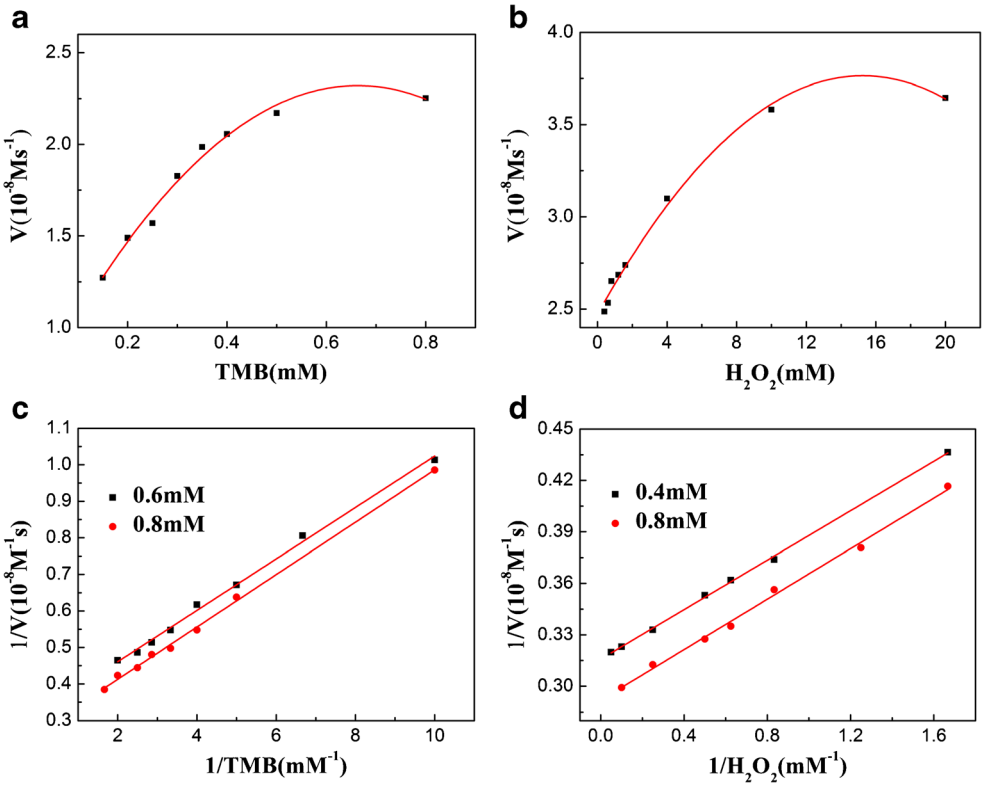

Fig. 3 Steady-state dynamic analysis of Fe_3O_4-Cu^{2+} NPs: Michaelis-Menten model with the H_2O_2 concentration of 0.4 mM and variation TMB concentration (**a**) and 0.25 mM TMB concentration and variation H_2O_2 concentration (**b**). (**c** and **d**) This is a double reciprocal plot of the activity of a variable concentration of Fe_3O_4-Cu^{2+} nanoparticles with the substrate (H_2O_2 or TMB) fixed concentration and another substrate

experimental conditional were found to give best results: (a) Best Sample pH value: 3.0; (b) Optimal reaction temperature: 45 °C; (c) Optimal Fe_3O_4-Cu^{2+} NP concentration:10 μg mL^{-1}; (d) Optimal reaction time: 35 min.

Kinetics analysis

The Michaelis-Menten constant (K_m) and maximum initial velocity (V_m) are the main kinetic parameters in regard to the catalytic rate and the binding affinity of the enzyme and zymolyte. Therefore, for the affinity between the enzyme and the substrate, we usually use the K_m value to represent. The binding affinity of the enzyme to the substrate becomes stronger as the value becomes smaller. In order to further research the catalytic mechanism of Fe_3O_4-Cu^{2+} NPs, enzyme kinetic theory was employed. First, the absorbance at 652 nm was recorded through changing the H_2O_2 or TMB concentration while maintaining the other concentration. Typical Michaelis-Menten plots in line with the Michaelis-Menten equation are achieved as shown in Fig. 3a and b. By means of Lineweaver-Burk port, in Table 1, we can determine and record K_m and V_m. The K_m data of the nanoparticles which had TMB as the substrate is 0.220 mM which is two times less than HRP, showing a higher binding affinity toward TMB peroxidase-like activity. In addition, the corresponding K_m value based on H_2O_2 is 0.228 mM which 16 and 675 times lower than the HRP and single Fe_3O_4, demonstrating a stronger binding affinity toward H_2O_2. These results clearly prove that the Fe_3O_4-Cu^{2+} NPs have super peroxidase-like activity. The reason may be ascribed to the synergistic effects from the nanoparticles structure, Fe_3O_4, and Cu^{2+} which can provide more active sites. Furthermore, we calculated the original speeds in the H_2O_2 or TMB range and drew a double reciprocal plot of the original speed versus another concentration of substrate. We can get parallel lines as reported in Fig. 3c and d. It suggests that the catalytic process

Table 1 Comparison of the K_m and V_{max} parameters of Fe_3O_4-Cu^{2+} nanoparticles with other reported nanozymes and HRP

Catalyst	Substance	K_m [mM]	V_{max} [10^{-8} Ms.$^{-1}$]	Ref.
GO–Fe_3O_4	TMB	0.43	13.08	[30]
	H_2O_2	0.71	5.31	
RhNPs	TMB	0.198	6.78	[31]
	H_2O_2	0.38	0.241	
Fe_3O_4	TMB	0.098	3.4	[32]
	H_2O_2	154	9.8	
HRP	TMB	0.43	10	[32]
	H_2O_2	3.7	8.71	
Fe_3O_4- Cu^{2+}	TMB	0.220	3.124	This work
	H_2O_2	0.228	3.166	

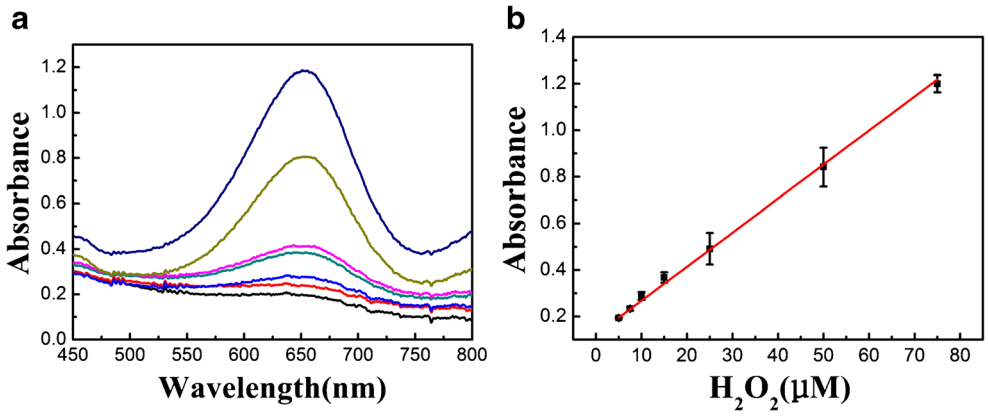

Fig. 4 **a** Spectra of UV-visible absorption of ox-TMB at variant H_2O_2 concentrations using Fe_3O_4-Cu^{2+} NPs being artificial enzymes. **b** This is a linear calibration plot that is consistent with H_2O_2 (the absorbance value at 652 nm was used)

of Fe_3O_4-Cu^{2+} NPs was in the light of the ping-pong mechanism, and the ping-pong was the mechanism of the multi-substrate enzyme reaction, the substrate and product are alternately bound to the enzyme or released from the enzyme and the process of HRP was also the same. This means combine and then they react with the first substrate, which release the reaction product and then react with the second substrate.

Detection of H_2O_2

To further verify the practical application of Fe_3O_4-Cu^{2+} NPs, a colorimetric means was used to detect the concentration of H_2O_2. Spectra of UV-visible absorption of ox-TMB at variants H_2O_2 concentrations using Fe_3O_4-Cu^{2+} NPs as artificial enzymes were recorded in Fig. 4. The absorbance in the condition of 652 nm is linearly rose with H_2O_2 concentration from 2.5 to 100 μM. The equation of linear regression is $A = 0.01461C + 0.12198$ (μM). What's more, the correlation coefficient is 0.99545 ($n = 3$). And the detection limit is 0.212 μM (3δ/S). The property of Fe_3O_4-Cu^{2+} NPs based H_2O_2 nanoprobe is compared to other materials which were reported previously (Table 2). It shows that the Fe_3O_4-Cu^{2+} NPs-based method possesses higher sensibility and better range of linearity that can enable it to detect H_2O_2 at μM levels. And in the actual detection process, the shortcomings of high reaction temperature limit their practical use.

Table 2 Comparison of linear range and detection limit obtained by different H_2O_2 method

Catalyst	Linear range	Detection limit	Ref.
GO-Fe_3O_4	1–50 μM	0.32 μM	[30]
Fe_3O_4@Au-PB	5.0 μM-5.0 mM	1.27 μM	[27]
Au/Pt NRs	1–250 μM	0.04 μM	[28]
CuNCs	10–1000 μM	10 μM	[33]
FePt-Au	20–700 μM	12.33 μM	[34]
Fe_3O_4-Cu^{2+}	2.5–100 μM	0.212 μM	This work

Selectivity of the method

This nanoprobe was tested for selectivity by conducting control experiments with some nonspecific species, including ascorbic acid (AA), citric acid (CA), dopamine (DA), K^+, Ca^{2+}, and Na^+. In. Figure 5, the absorbance of these systems at 652 nm and relative color change were reported. Maximum absorbance intensity and a deep blue color were obtained in the presence of H_2O_2 while the value was tiny for others. The results proved that the nanoprobe system exhibited good selectivity to H_2O_2.

Conclusion

A two-stage process is presented to prepare copper(II)-coated Fe_3O_4 magnetic nanoparticles. Taking TMB as an example, the Fe_3O_4-Cu^{2+} NPs possessed super peroxidase-like mimic properties in terms of catalytic active centers and substrate binding sites. The catalytic property of the NPs is related with pH, temperature, material concentration, and reaction time. The catalytic activity conformed to the Michaelis-Menten model, and the enzyme catalytic reaction was in line with the ping-pong mechanism. Compared to HRP, the NPs had excellent durability and thermal stability. Moreover, the

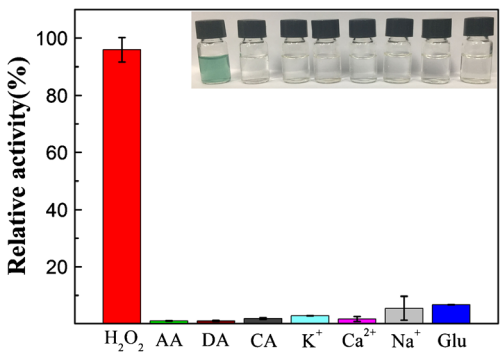

Fig. 5 Relative activity of the Fe_3O_4-Cu^{2+} NPs system with H_2O_2, AA, DA, CA, K^+, Ca^{2+}, Na^+, and glucose. Inset: color changes associated with variant hierarchy

property of NPs is much higher than HRP and some reported nanozymes. On these bases, an ingenious colorimetric H_2O_2 nanoprobe was successfully devised by using the intrinsic HRP-like activity of the NPs. So, we have achieved a satisfactory archive of linear range and lower detection limit. Thus, we anticipate that the magnetic Fe_3O_4-Cu^{2+} NPs have potential application in terms of food security, ecological protection, and biomedical diagnosis.

Acknowledgements This study was financed by the Science and Technology Program of Zhejiang Province of China (LGF18H200005), NSFC (21405029, and 61731008), the Medical and Health Technology Development Program of Zhejiang province (2017KY533), and the Young and Middle-aged Academic Leaders of Zhejiang Province.

Compliance with ethical standards The author(s) declare that they have no competing interests.

References

1. Rhee SG (2006) Cell signaling. H_2O_2, a necessary evil for cell signaling. Science 312:1882–1883
2. Li C, Wang S, Huang Y, Wen Q, Kan Y (2014) Photoluminescence properties of a novel cyclometalated iridium (III) complex with coumarin-boronate and its recognition of hydrogen peroxide. Dalton T 43(14):5595–5602
3. Lee M, Patil V, Na Y, Lee D, Lim S, Yi G (2018) Highly stable, rapid colorimetric detection of carbaryl pesticides by azo coupling reaction with chemical pre-treatment. Sensors Actuat B-Chem 261: 489–496
4. Nasir M, Nawaz MH, Yaqub M, Hayat A, Rahim A (2017) An overview on enzyme-mimicking nanomaterials for use in electrochemical and optical assays. Microchim Acta 184(2):323–342
5. Gao L, Zhuang J, Nie L, Zhang J, Zhang Y, Gu N, Wang T, Feng J, Yang D, Perrett S, Yan X (2007) Intrinsic peroxidase-like activity of ferromagnetic nanoparticles. Nat Nanotechnol 2(9):577–583
6. Zhang Z, Wang Z, Wang X, Yang X (2010) Magnetic nanoparticle-linked colorimetric aptasensor for the detection of thrombin. Sensors Actuat B-Chem 147(2):428–433
7. Safarik I, Safarikova M (2004) Magnetic techniques for the isolation and purification of proteins and peptides. Biomagn Res Technol 2:1–17
8. Ito A, Hibino E, Kobayashi C, Terasaki C, Kagami H, Ueda M, Kobayashi T, Honda H (2005) Construction and delivery of tissue-engineered human retinal pigment epithelial cell sheets, using magnetite nanoparticles and magnetic force. Tissue Eng A 11:489–496
9. Ding C, Yan Y, Xiang D, Zhang C, Xian Y (2016) Magnetic Fe_3S_4, nanoparticles with peroxidase-like activity, and their use in a photometric enzymatic glucose assay. Microchim Acta 183:625–631
10. Lin T, Lin F, Lin J (2012) In vitro feasibility study of the use of a magnetic electrospun chitosan nanofiber composite for hyperthermia treatment of tumor cells. Acta Biomater 8:2704–2711
11. Jiang Y, Jiang J, Gao Q, Ruan M, Yu H, Qi L (2008) A novel nanoscale catalyst system composed of nanosized Pd catalysts immobilized on Fe_3O_4@SiO_2-PAMAM. Nanotechnol. 19:075714
12. Wang J, Yang X, Li A, Cai X (2018) Preparation and characterization of multifunctional Fe_3O_4-coated Ag nanocomposites for catalytic reduction of 4-nitrophenol. Mater Lett 220:24–27
13. Pham V, Kim D, Ko S (2017) Cu@Fe_3O_4, core-shell nanoparticle-catalyzed oxidative degradation of the antibiotic oxytetracycline in pre-treated landfill leachate. Chemosphere 191:639–650
14. Yu X, Wan J, Shan Y, Chen K, Han X (2009) A facile approach to fabrication of bifunctional magnetic-optical Fe_3O_4@ZnS microspheres. Chem Mater 21:4892–4898
15. Vazquez-Gonzalez M, Liao W, Cazelles R, Wang S, Yu X, Gutkin V, Willner I (2017) Mimicaking horseradish peroxidase functions using Cu^{2+} modified carbon nitride nanoparticles or Cu^{2+}-modified carbon dots as heterogeneous catalysts. ACS Nano 11:3247–3253
16. Wang S, Cazelles R, Liao W, Vazquez-Gonzalez M, Zoabi A, Reziq R, Willner I (2017) Mimicaking horseradish peroxidase and NADH peroxidase by heterogenous Cu-modified graphene oxide nanoparticles. Nano Lett 17:2043–2048
17. Chen W, Vazquez-Gonzalez M, Kozell A, Cecconello A, Willner I (2018) Cu^{2+}-modified metal-organic framework nanoparticles: a peroxidase-mimicking nanoenzyme. Small 14:1703149–1703156
18. Wang Z, Chen Y, Dong W, Zhou J, Han B, Jiao J, Lan L, Miao P, Chen Q (2018) Copper(II)-poly-L-histidine functionalized multi walled carbon nanotubes as efficient mimetic enzyme for sensitive electrochemical detection of salvianic acid A. Biosens Bioelectron 121:257–264
19. Xiong Y, Qin Y, Su L, Ye F (2017) Bioinspired synthesis of Cu^{2+}-modified covalent triazine framework: a new highly efficient and promising peroxidase mimic. Chem Eur J 23:1–10
20. Liang H, Lin F, Zhang Z, Liu B, Jiang S, Yuan Q, Liu J (2016) Multi-copper laccase mimicking nanozymes. ACS Appl Mater Interfaces 9:1352–1360
21. Qin Y, Li Y, Liu X, Lu Z, Zheng L, Liu S, Cao Q, Ding Z (2017) Copper metal-organic polyhedral nanorods with high intrinsic peroxidase activity at physiological pH for bio-sensing. J Mater Chem B 5:9365–9370
22. Menon S, Chandran S, Koyappayil A, Berchmans S (2018) Copper-based metal-organic frameworks as peroxidase mimics leading to sensitive H_2O_2 and glucose detection. Chem Select 3: 8319–8324
23. Luo C, Wang X, Wang J, Pan K (2016) One-pot preparation of polyimide/Fe_3O_4, magnetic nanofibers with solvent resistant properties. Compos Sci Technol 133:97–103
24. Wang Y, Wang X, Ding Y, Zhou Z, Hao C, Zhou Z (2018) Novel sodium lignosulphonate assisted synthesis of well dispersed Fe_3O_4, microspheres for efficient adsorption of copper(II). Powder Technol 325:597–605
25. Guo J, Wang Y, Zhao M (2018) 3D flower-like ferrous(II) phosphate nanostructures as peroxidase mimetics for sensitive colorimetric detection of hydrogen peroxide and glucose at nanomolar level. Talanta 182:230–240
26. Lin Y, Chang Y, Chen G, Chang Y (2009) Effects of Ag-doped $NiTiO_3$ on photoreduction of methylene blue under UV and visible light irradiation. J Alloys Compd 479:785–790
27. Li Y, Li J, Fu Y, Xie Q, Li Y (2019) Magnetic-core@dual-functional-shell nanocomposites with peroxidase mimicking properties for use in colorimetric and electrochemical sensing of hydrogen peroxide. Microchim Acta 186(1):20–28
28. Sun Y, Wang R, Liu X, Shan G, Chen Y, Tong T, Liu Y (2018) Laser-induced formation of Au/Pt nanorods with peroxidase mimicking and SERS enhancement properties for application to the colorimetric determination of H_2O_2. Microchim Acta 185(9):445–454
29. Wang N, Duan J, Shi W, Zhai X, Guan F, Yang L, Hou B (2018) A 3-dimensional C/CeO_2 hollow nanostructure framework as a peroxidase mimetic, and its application to the colorimetric determination of hydrogen peroxide. Microchim Acta 185(9):417–425
30. Dong Y, Zhang H, Rahman Z, Su L, Chen X, Hu J, Chen X (2012) Graphene oxide-Fe_3O_4 magnetic nanocomposites with peroxidase-like activity for colorimetric detection of glucose. Nanoscale 4: 3969–3976
31. Choleva TG, Gatselou VA, Tsogas GZ, Giokas DL (2018) Intrinsic peroxidase-like activity of rhodium nanoparticles, and their

application to the colorimetric determination of hydrogen peroxide and glucose. Microchim Acta 185(1):22

32. Gao L, Zhuang J, Nie L, Zhang J, Zhang Y, Gu N, Wang T, Feng J, Yang D, Perrett S (2007) Intrinsic peroxidase-like activity of ferromagnetic nanoparticles. Nat Nanotechnol 2:577–583
33. Hu L, Yuan Y, Zhang J, Zhao J, Majeed S, Xu G (2013) Copper nanoclusters as peroxidase mimetics and their applications to H_2O_2 and glucose detection. Anal Chim Acta 762:83–86
34. Ding Y, Yang B, Liu H, Liu Z, Zhang X, Zheng X, Liu Q (2018) FePt-Au ternary metallic nanoparticles with the enhanced peroxidase-like activity for ultrafast colorimetric detection of H_2O_2. Sensors Actuators B Chem 259:775–783

Publisher's note Springer Nature remains neutral with regard to jurisdictional claims in published maps and institutional affiliations.